

Synthesis, characterization crystal structures and DNA binding studies of zinc complexes with oxygen and nitrogen donor ligands



Mehr-un-Nisa^a, Muhammad Sirajuddin^{b,*}, Saqib Ali^{a,*}, Muhammad Nawaz Tahir^c, Muhammad Iqbal^{d,*}

^a Department of Chemistry, Quaid-I-Azam University, Islamabad 45320, Pakistan

^b Department of Chemistry, University of Science & Technology, Bannu 28100, KP, Pakistan

^c Department of Physics, University of Sargodha, Sargodha, Pakistan

^d Department of Chemistry, Bacha Khan University, Charsadda, Pakistan

ARTICLE INFO

Article history:

Received 29 October 2019

Accepted 27 November 2019

Available online 18 December 2019

Keywords:

Zn(II) complexes

Crystal structure

FR-IR

NMR

DNA binding study

ABSTRACT

Three zinc metal complexes viz, $[Zn(L^1)_2phen]$ (**1**), $[Zn_2(L^2)_4(bipy)_2]$ (**2**) and $[Zn(L^2)_2bipy \cdot H_2O]$ (**3**) where $HL^1 = 4-(o\text{-toluidino})\text{-4-oxobutanoic acid}$ and $HL^2 = 4\text{-}(4\text{-nitrophenyl amino})\text{-4-oxobut-2-enoic acid}$, $bipy = 2,2\text{-bipyridine}$ and $phen = 1,10\text{-phenanthroline}$. To elucidate their structure and geometry, the synthesized complexes were characterized by different analytical techniques such as FT-IR, 1H NMR, ^{13}C NMR and single crystal X-ray diffraction analysis. Single crystal X-ray analysis confirmed slightly distorted square pyramidal geometry for complex **2** and distorted octahedral geometry for complexes **1** and **3**. To explore the applications of synthesized complexes, their DNA binding studies were performed by viscometry and UV-Visible spectroscopy. By using these techniques, binding constants with DNA and Gibb's free energy change was calculated of synthesized complexes. All the complexes showed spontaneous binding with DNA with K_b values 7.05×10^4 , 1.06×10^4 , $1.6 \times 10^4 M^{-1}$ and the Gibb's free energy $\Delta G = -27.6$, -22.9 and $-23.8 kJmol^{-1}$, respectively for complexes **1-3**.

© 2019 Elsevier Ltd. All rights reserved.

1. Introduction

Metal complexes have fascinating coordination chemistry, remarkable physical and chemical properties, structural diversity and wide applications as extractants, drugs, dyes, pesticides and catalysts [1–4]. There is a variety or diversity in structures of metal-organic coordination complexes due to several factors such as counter ions [5], reaction temperature [6], coordination mode of metal ion [7], pH [8] solvent [9] and metal-to-ligand ratio [10]. The carboxylate ligands have different coordination modes such as monodentate, bidentate, tridentate, bridging and chelating [11]. These ligands play an important role to form supra-molecular structures of the complexes [12].

Zinc has many applications in the field of biology, industries, medicine and agriculture. Zinc has some antioxidant properties which may protect the body muscles and skin from aging [13]. Zinc complexes with a variety of nitrogen donor ligands have many

applications in different areas of chemistry such as solution, surface and redox chemistry [14–17].

DNA is the primary target of many anticancer drugs due to its prime role in cell life. It is highly important to know the interaction mode of the anticancer drug as DNA offers a number of interactive sites for covalent and non-covalent binders. Zinc complexes are the favorable candidates for DNA binding as well as for its cleavages [18]. The synthesis of new compounds with better binding affinity like *cis*-platin is the demand of the day for nucleic acid structures [19]. The study of the interaction of transition metal complexes with DNA has been the main focus of recent research. Subsequent structural changes in a DNA strands can easily be examined by a number of experimental techniques [20].

Among the *N*-donor ligands, 2,2'-bipyridine and 1,10-phenanthroline are biologically important ligands having chelating nature as well as planar structure. Such ligands possess good coordinating ability due to π - π interactions and thus their use for complexation import enhancement in various chemical and biological properties [16,17].

In the present study, three Zn(II) mixed ligand complexes have been synthesized and characterized by various spectroscopic techniques. Both shows a remarkable DNA interactions and the results of DNA binding in UV Visible spectroscopy have been correlated with viscometry.

* Corresponding authors.

E-mail addresses: m.siraj09@gmail.com (M. Sirajuddin), drsa54@hotmail.com (S. Ali), iqbal@bkcuc.edu.pk (M. Iqbal).

2. Experimental

2.1. Materials

4-Nitroaniline, *o*-toluidine, maleic anhydride, succinic anhydride, acetic acid, $\text{Zn}(\text{CH}_3\text{COO})_2 \cdot 2\text{H}_2\text{O}$, NaHCO_3 , 1,10-phenanthroline and 2,2'-bipyridine were acquired from Aldrich and used as such. Solvents like methanol, DMSO were purchased from Merck, Germany and used as such without further purification. Distilled water was used for washing of precipitates and salt solutions preparation.

2.2. Physical measurements

Capillary tubes were used for determining melting points in an electro thermal melting point apparatus model MP-D Mitamura Riken Kogyo (Japan). FT-IR spectra were obtained in the range of 4000–400 cm^{-1} using Nicolet-6700 FT-IR spectrophotometer. ^1H and ^{13}C NMR were determined at room temperature using DMSO as an internal reference on a Bruker Advance Digital 300 MHz NMR spectrometer (Switzerland). Analyses of X-ray single crystal were performed using Bruker Kappa APEXII CCD diffractometer using graphite-monochromated Mo- $\text{K}\alpha$ radiation ($\lambda = 0.71073 \text{ \AA}$). Crystal structures were solved by using direct method followed by final refinement carried on F^2 with full-matrix least-squares using the program SHELXL-97 [21]. The Hydrogen atoms were treated as riding atoms and included in calculated positions; C–H = 0.93, 0.96 and 0.97 \AA for CH , CH_3 and CH_2 H-atoms, respectively, with $U_{\text{iso}}(\text{H}) = kU_{\text{eq}}(\text{C})$, where $k = 1.5$ for CH_3 and 1.2 for all other H-atoms. DNA interactions studies were done using UV-Visible spectroscopy on a Beckman U-2020 spectrophotometer and Ubbelohde viscometer.

2.3. Synthesis of the ligands HL^1 and HL^2

The ligand HL^1 (4-(*o*-toluidino)-4-oxobutanoic acid) was prepared by treating the equimolar quantities *o*-toluidine with succinic anhydride in glacial acetic acid at room temperature. Similarly HL^2 (4-(4-nitrophenyl amino)-4-oxobut-2-enoic acid) was prepared from the reaction of equimolar quantities *p*-nitroaniline with maleic anhydride in glacial acetic acid at room temperature [22].

2.4. Synthesis of the complexes 1–3

2.4.1. $[\text{Zn}(\text{L}^1)_2\text{phen}]$ (Complex 1)

The sodium salt of HL^1 was prepared by the reaction of HL^1 (4 mmol) suspended in distilled water with the aqueous solution of sodium bicarbonate (4 mmol) with constant stirring at room temperature [22]. The reaction mixture was stirred to get the clear solution. Then aqueous solution of zinc nitrate hexahydrate (2 mmol) was added dropwise to the reaction mixture followed by the addition of 1,10-phenanthroline (2 mmol dissolved in little methanol) and stirred at 40 $^\circ\text{C}$ for 3–4 h. The resulting desired white precipitates of complex 1 were filtered, washed with distilled water and then air dried.

2.4.2. $[\text{Zn}_2(\text{L}^2)_4(\text{bipy})_2]$ (Complex 2) and $[\text{Zn}(\text{L}^2)_2(\text{bipy})(\text{H}_2\text{O})]$ (Complex 3)

Sodium salt of HL^2 was prepared by similar way as that of HL^1 explained in the synthesis procedure of complex 1. 2,2'-bipyridine (2 mmol) was used instead of 1,10-phenanthroline and resulting desired light yellow and half white precipitates of complexes 2 and 3, respectively were appeared which were filtered, washed

with distilled water and then air dried. Complex 2 was crystallized in DMSO while complex 3 in methanol.

2.4.3. HL^1

$^1\text{H NMR}$ (DMSO d_6 , 300 MHz) δ (ppm): 12.12 (s, 1H), 2.58 (t, 2H, H2, $^3J[^1\text{H}, ^1\text{H}] = 6.9 \text{ Hz}$); 2.54 (t, 2H, H3, $^3J[^1\text{H}, ^1\text{H}] = 6.9 \text{ Hz}$); 9.29 (s, 1H NH); 7.38 (d, $^3J[^1\text{H}, ^1\text{H}] = 7.5 \text{ Hz}$, 1H, H6); 7.20 (m, 2H, H7 and H8); 7.34 (d, 1H, H9, $^3J[^1\text{H}, ^1\text{H}] = 7.2 \text{ Hz}$); 2.18 (s, 3H, H11); $^{13}\text{C NMR}$ (DMSO d_6 , 75 MHz) δ (ppm): 174.4 (C1); 31.0 (C2); 29.67 (C3); 170.5 (C4); 137.5 (C5); 126.3 (C6); 125.4 (C7); 130.7 (C8); 132.1 (C9), 136.8 (C10), 18.3 (C11).

2.4.4. Complex 1

$^1\text{H NMR}$ (DMSO d_6 , 300 MHz) δ (ppm): 2.58 (t, 2H, H2, $^3J[^1\text{H}, ^1\text{H}] = 6.9 \text{ Hz}$); 2.54 (t, 2H, H3, $^3J[^1\text{H}, ^1\text{H}] = 6.9 \text{ Hz}$); 9.29 (s, 1H NH); 7.38 (d, $^3J[^1\text{H}, ^1\text{H}] = 7.5 \text{ Hz}$, 1H, H6); 7.20 (m, 2H, H7 and H8); 7.34 (d, 1H, H9, $^3J[^1\text{H}, ^1\text{H}] = 7.2 \text{ Hz}$); 2.18 (s, 3H, H11); {8.85 (d, 1H, $^3J[^1\text{H}, ^1\text{H}] = 7.8 \text{ Hz}$); 8.00 (m, 1H); 8.48 (m, 1H); 9.07 (s, 1H) (1,10-phenanthroline H)}; $^{13}\text{C NMR}$ (DMSO d_6 , 75 MHz) δ (ppm): 179.0 (C1); 33.1 (C2); 31.8 (C3); 171.4 (C4); 140.1 (C5); 126.0 (C6); 125.0 (C7); 126.2 (C8); 127.4 (C9), 136.8 (C10), 18.2 (C11); {150.0, 125.0, 128.8, 127.4, 123.0, 140.4 (1,10-phenanthroline C)}.

2.4.5. HL^2

$^1\text{H NMR}$ (DMSO d_6 , 300 MHz) δ (ppm): 12.79 (s, 1H), 6.51 (d, 1H, H2, $^3J[^1\text{H}, ^1\text{H}] = 12 \text{ Hz}$); 6.37 (d, 1H, H3, $^3J[^1\text{H}, ^1\text{H}] = 12 \text{ Hz}$); 10.86 (s, 1H NH); 7.87 (d, 2H, H6,6', $^3J[^1\text{H}, ^1\text{H}] = 9 \text{ Hz}$); 8.25 (d, 2H, H7,7', $^3J[^1\text{H}, ^1\text{H}] = 9 \text{ Hz}$); $^{13}\text{C NMR}$ (DMSO d_6 , 75 MHz) δ (ppm): 169.6 (C1); 138.6 (C2); 130.3 (C3); 163.2 (C4); 142.0 (C5); 121.3 (C6,6'); 122.5 (C7,7'); 144.0 (C8).

2.4.6. Complex 2

$^1\text{H NMR}$ (DMSO d_6 , 300 MHz) δ (ppm): 6.26 (d, 1H, H2, $^3J[^1\text{H}, ^1\text{H}] = 12 \text{ Hz}$); 6.12 (d, 1H, H3, $^3J[^1\text{H}, ^1\text{H}] = 12 \text{ Hz}$); 12.2 (s, 1H NH); 7.85 (d, 2H, H6,6', $^3J[^1\text{H}, ^1\text{H}] = 7.2 \text{ Hz}$); 8.18 (d, 2H, H7,7', $^3J[^1\text{H}, ^1\text{H}] = 7.2 \text{ Hz}$); {8.66 (d, 1H, $^3J[^1\text{H}, ^1\text{H}] = 5.2 \text{ Hz}$); 7.93 (m, 1H); 7.70 (m, 1H); 9.2 (d, 1H, $^3J[^1\text{H}, ^1\text{H}] = 5.2 \text{ Hz}$) (2,2'-Bipyridine H)}; $^{13}\text{C NMR}$ (DMSO d_6 , 75 MHz) δ (ppm): 170.5 (C1); 135.3 (C2); 130.1 (C3); 163.8 (C4); 141.4 (C5); 119.1 (C6,6'); 125.4 (C7,7'); 142.4 (C8); {145.8, 127.0, 136.9, 122.4, 149.3 (2,2'-Bipyridine C)}.

2.4.7. Complex 3

$^1\text{H NMR}$ (DMSO d_6 , 300 MHz) δ (ppm): 6.32 (d, 1H, H2, $^3J[^1\text{H}, ^1\text{H}] = 12.6 \text{ Hz}$); 6.06 (d, 1H, H3, $^3J[^1\text{H}, ^1\text{H}] = 12.9 \text{ Hz}$); 13.12 (s, 1H NH); 7.75 (d, 2H, H6,6', $^3J[^1\text{H}, ^1\text{H}] = 7.0 \text{ Hz}$); 8.19 (d, 2H, H7,7', $^3J[^1\text{H}, ^1\text{H}] = 7.0 \text{ Hz}$); {8.75 (d, 1H, $^3J[^1\text{H}, ^1\text{H}] = 6.3 \text{ Hz}$); 8.28 (m, 1H); 7.71 (m, 1H); 8.64 (d, 1H, $^3J[^1\text{H}, ^1\text{H}] = 6.3 \text{ Hz}$) (2,2'-Bipy H)}; 3.32 (s, H of water molecule); $^{13}\text{C NMR}$ (DMSO d_6 , 75 MHz) δ (ppm): 171.3 (C1); 136.9 (C2); 130.4 (C3); 164.8 (C4); 141.3 (C5); 119.1 (C6,6'); 125.5 (C7,7'); 142.4 (C8); {145.9, 127.0, 136.9, 124.7, 149.3 (2,2'-Bipyridine C)}.

2.5. DNA interaction study by UV-Visible spectroscopy

The commercially available salmon sperm DNA was dissolved in distilled water and kept at 4 $^\circ\text{C}$ for 4 days. During the interaction study of DNA with complex molecules, the changes or shifting in the absorption peaks were monitored. DNA shows maximum absorption peak at 260 nm. The nucleotide to protein ratio in the range of 1.8–1.9 was calculated by the absorbance ratios (A_{260}/A_{280} and A_{260}/A_{230}) which showed the DNA was free from protein molecules [22]. The concentration of DNA was determined through absorption spectroscopy by using the value of molar absorption coefficient, i.e., $6600 \text{ M}^{-1} \text{ cm}^{-1}$ (at 260 nm) and calculated to be

$5.5 \times 10^{-5} \text{ M}^{-1}$. Working solutions were prepared from this stock solution by dilution method. The complex solutions of concentrations 0.5 mM were prepared in DMSO. During UV absorption measurements concentration of complexes were kept constant while DNA concentration was varied. Equivalent concentration of DNA was added to the reference and sample cells to cancel the effect of DNA absorbance so that DNA itself does not show any absorbance. Quartz cells having 1 cm path length were used for recording absorption spectra at room temperature. Before recording the next spectrum, quartz cells were rinsed with acetone and air dried.

Benesi-Hildebrand's equation [23] was used for calculating the value of drug-DNA binding constant and Gibb's free energy (ΔG) was calculated to check the spontaneity of drug-DNA binding processes.

2.6. Viscosity measurements

Ubbelohde viscometer was used for measuring viscosity at room temperature. Flow time was measured by using digital stopwatch. At least three readings were taken and average flow time was measured. After each measurement viscometer was rinsed with acetone and oven dried, using this method η and η_0 was calculated and graph was plotted between $(\eta/\eta_0)^{1/3}$ and [compound]/[DNA] concentration ratio, where η is the viscosity of DNA in the presence of drug whereas η_0 is the viscosity of free DNA without any drug [24]. Viscosity was calculated from the observed flow time of DNA containing solution (t_0): $\eta_0 = t - t_0$ [25].

3. Results and discussion

The physical data including color, physical state, melting point, molecular weight, solubility and percentage yield of the synthesized compounds are given in Table 1.

3.1. FT-IR data

The characteristics FT-IR peaks for the synthesized compounds are shown in Table 2. There are two possibilities for carboxylate ligand to bind to a central metal ion, either in monodentate or bidentate mode. In Zn-carboxylates it can adopt both types of bonding modes [26]. The carboxylate moiety showed $\nu\text{OCO}_{\text{asym}}$ bands at 1540, 1587 and 1580 cm^{-1} while $\nu\text{OCO}_{\text{sym}}$ bands at 1432, 1382 and 1374 cm^{-1} for complexes 1–3, respectively. The

$\Delta\nu = \{\nu\text{OCO}_{\text{asym}} - \nu\text{OCO}_{\text{sym}}\}$ calculated for complex 1 are 114 cm^{-1} indicating a bidentate coordination mode of carboxylate moiety while for complex 3, the value of $\Delta\nu$ is 206 cm^{-1} , respectively indicating a monodentate coordination mode of carboxylate groups [27]. In complex 2 two types of bands regarding asymmetric and symmetric stretching vibrations of carboxylate ligands were observed which are $\nu\text{OCO}_{\text{asym}}$ ($1550, 1720 \text{ cm}^{-1}$) and $\nu\text{OCO}_{\text{sym}}$ ($1374, 1365 \text{ cm}^{-1}$). The $\Delta\nu$ values are (176 and 355 cm^{-1}), suggesting both bidentate bridging and monodentate type of bonding modes of ligands co-existing in solid state [28,29]. The broad band at 3451 cm^{-1} is attributed to OH of water molecules in complex 3. The NH- group showed absorption bands at 3322, 3340 and 3343 cm^{-1} for complexes 1–3. The absorption bands observed in the range $417\text{--}428 \text{ cm}^{-1}$ correspond to Zn–O cm^{-1} of the complexes. The bands at 513, 531 and 527 cm^{-1} are attributed to the Zn–N vibrations [30] of the complexes 1–3.

3.2. NMR data

^1H and ^{13}C NMR chemical shifts of ligands and their complexes are presented in experimental section while the numbering scheme of the ligands has been given in Scheme 1 while the representative ^1H and ^{13}C NMR spectra are given in supplementary data (Figs. S1–S4). A comparative NMR analysis gives evidence for the complex formation and the ligand coordination with metal ion. In ligands, a sharp peak appears in the region 10–12 ppm due to OH group of acids and after complexation this OH peak disappeared. In ^1H NMR spectra aromatic protons appeared in the region 6.5–8.75 ppm showing multiplets. At 6.3–6.55 ppm olefinic protons appeared. Their value of coupling constant was calculated to be 12 which indicate that these protons are *trans* to each other. The peaks of 1,10-phenanthroline and 2,2'-bipyridine were appeared in their respective regions. In complex 3, the peak observed at 3.32 ppm confirms the coordination of water molecule [30].

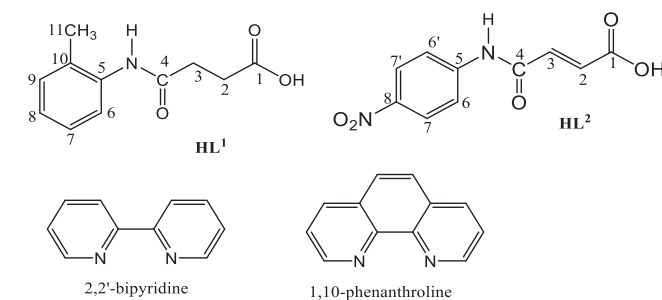
In the ^{13}C NMR of the ligands spectra, the signals at 174.3 ppm (HL^1) and 169.6 ppm (HL^2) were assigned to the carboxylate C1 carbons. The signal of C1 is more sensitive to environmental changes than other carbon atoms so after complexation it became deshielded and shifted to downfield region. The acquired data showed shifting of the C1 signal upon complexation to 179 ppm in complex 1 and 170.5–171.3 ppm in complexes 2 and 3. This

Table 1
Physical data of HL^1 , HL^2 and their Zinc(II) complexes.

Compounds	Color	Physical State	Melting Point (°C)	Mol. Wt.	Solubility	% Yield
HL^1	White	Solid	165–167	207	DMSO	82
$\text{Zn}(\text{L}^1)_2\text{phen}$ (1)	White	Solid	208–210	657	DMSO	77
HL^2	Yellow	Solid	156–158	236	DMSO	79
$\text{Zn}(\text{L}^2)_4(\text{bipy})_2$ (2)	Light yellow	Solid	204–206	1496	DMSO	79
$\text{Zn}(\text{L}^2)_2\text{bipyH}_2\text{O}$ (3)	Half white	Solid	189–191	644	DMSO	75

Table 2
FT-IR data (cm^{-1}) of HL^1 , HL^2 and their Zn(II) complexes.

Comp.#	νOH	νNH	νCO	$\nu\text{COO}_{\text{asym}}$	$\nu\text{COO}_{\text{sym}}$	$\Delta\nu$	$\nu\text{C}=\text{C}$	$\nu\text{Zn-O}$	$\nu\text{Zn-N}$
HL^1	3442	3326	1693	1657	1530	–	–	–	–
1	–	3322	1661	1546	1432	114	–	428	513
HL^2	3425	3345	1702	1623	1431	–	1645	–	–
2	–	3340	1679	1550, 1720	1374, 1365	174,355	1632	417	531
3	3451	3343	1667	1560	1384	206	1627	420	527



Scheme 1. Numbering scheme of ligands for ^1H NMR and ^{13}C NMR data.

downfield shifting is due to the transfer of electron density from the ligands toward to electropositive Zn metal [30,31]. Additional signals were observed for the carbon atoms of 1,10-phenanthroline and 2,2'-bipyridine in their respective regions [30,31].

3.3. Single crystal X-ray analysis

3.3.1. Crystal structure of complex 1

The crystal structure of complex 1 is shown in Fig. 1 and structural parameters in Table 3. The selected bond angles and lengths are presented in Tables 4 and 5. In this complex the central metal atom zinc is coordinated with oxygens of two carboxylate ligands and with two nitrogen atoms of phenanthroline ligand. Both carboxylates and phenanthroline has a bidentate mode. The crystal system of this complex is triclinic with space group *P*-1. The geometry around the zinc is distorted octahedral due to the bulkiness or steric hindrance of the ligands and electron pair repulsion. The bond distance between nitrogens of 1,10-phenanthroline and zinc metal is asymmetric, Zn-N bond lengths are 2.07 and 2.11 Å. The bond angles between N₁ZnO₂ and N₂ZnO₄ are 146.11° and 138.2°, respectively which also confirms the distortion in octahedral geometry and the other bond angles and bond lengths are

Table 4
Selected bond lengths (Å) for complexes 1–3.

Complex 1			
Zn-O1	2.024	Zn-O5	2.197
Zn-O2	2.434	Zn-N1	2.118
Zn-O4	2.148	Zn-N2	2.076
Complex 2			
Zn1-O1	1.980(2)	Zn2-O16	1.979(2)
Zn1-O12	2.049(2)	Zn2-O11	2.030(2)
Zn1-O6	2.080(2)	Zn2-O7	2.040(2)
Zn1-N3	2.084(2)	Zn2-N10	2.119(2)
Zn1-N4	2.112(2)	Zn2-N9	2.135(2)
Complex 3			
Zn1-O6	2.008(2)	Zn2-O17	2.016(2)
Zn1-O11	2.030(2)	Zn2-O12	2.023(2)
Zn1-O1	2.038(2)	Zn2-O22	2.037(2)
Zn1-N1	2.106(2)	Zn2-N7	2.114(3)
Zn1-N2	2.114(2)	Zn2-N8	2.117(3)

given in Table 5. The structural parameters are found typical of the other structurally related zinc complex [30–33]. The two carboxylate ligands chelate to the zinc metal in an asymmetric manner as depicted by four different bond distances of Zn-O. Both

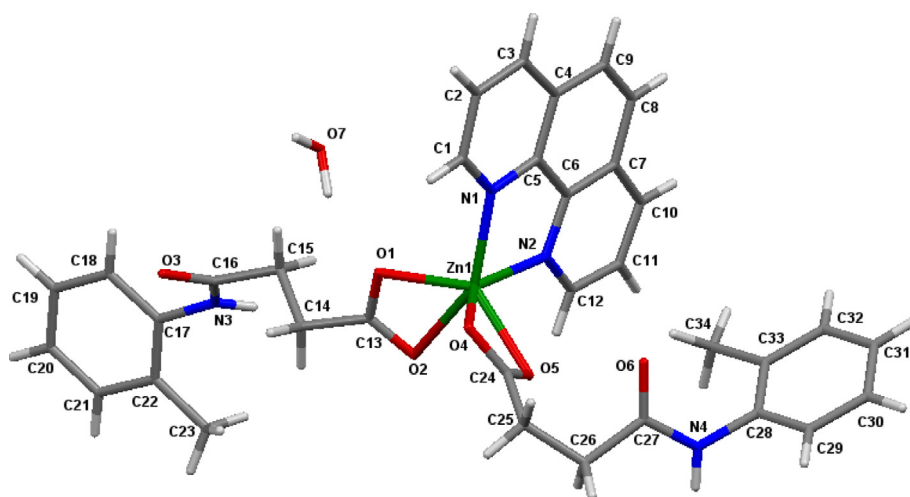


Fig. 1. Molecular diagram of complex 1.

Table 3
Crystal data and structure refinement parameters for complexes 1–3.

Refinement parameters	1	2	3
Chemical Formula	C ₂₆ H ₂₀ N ₄ O ₈ Zn	C ₆₂ H ₅₃ N ₁₂ O ₂₃ SZn ₂	C ₃₀ H ₂₄ N ₆ O ₁₁ Zn
Formula weight	657.02	1496.96	644.48
T(K)	296(2)	296(2)	296(2)
Wavelength (nm)	0.71073	0.71073	0.71073
Crystal system	triclinic	Orthorhombic	monoclinic
Space group	<i>P</i> -1	<i>P</i> b c a	<i>P</i> 2 ₁ / <i>c</i>
a/b/c(Å)	8.2179(3), 14.0016(6), 14.1707(6)	26.1556(10), 15.0546(4), 32.9176(13)	13.4790(4), 17.2382(6), 28.5319(9)
α/β/γ (°)	80.129(2), 80.231(3), 88.664(2)	90, 90, 90	90, 101.932(2), 90
V(Å ³)/Z	1583.08(11)/2	12961.7(8)/8	6486.3(4)/4
μ(mm ⁻¹)	0.831	0.863	0.834
F(0 0 0)	704	6152	3104
Crystal size (mm)	0.40 × 0.30 × 0.18	0.40 × 0.32 × 0.24	0.38 × 0.30 × 0.24
θ-range for data calculation	1.48 to 25.99	1.462 to 25.5	1.38 to 27.172
Reflection collected	6198	11,677	14,361
Independent reflection	5121	4025	8750
Goodness-of-fit on <i>F</i> ²	1.010	1.020	1.013
Final R indices [<i>I</i> > 2σ(<i>I</i>)]	R1 = 0.0436, wR2 = 0.0883	R1 = 0.0406, wR2 = 0.0901	R1 = 0.0953, wR2 = 0.1208
R indices (all data)	R1 = 0.0332, wR2 = 0.0817	R1 = 0.0713, wR2 = 0.1058	R1 = 0.0483, wR2 = 0.1208
Data/restraints/parameters	6198/0/423	11677/0 /925	14361/2/937
CCDC #	1951633	1959883	1951634

Table 5
Selected bond angles (°) for complexes 1–3.

Complex 1			
O1–Zn–O2	56.59	O2–Zn–N1	146.11
O1–Zn–O4	102.44	O2–Zn–N2	96.48
O1–Zn–O5	131.9	O4–Zn–N1	93.96
O2–Zn–O4	109.9	O4–Zn–N2	138.24
O2–Zn–O5	86.46	O5–Zn–N1	127.05
O4–Zn–O5	59.38	O5–Zn–N2	91.97
O1–Zn–N1	95.87	N1–Zn–N2	79.36
O1–Zn–N2	119.18	O1–Zn–N2	119.18
Complex 2			
O1–Zn1–O12	97.49(9)	O16–Zn2–O11	110.84(10)
O1–Zn1–O6	84.32(9)	O16–Zn2–O7	96.83(9)
O12–Zn1–O6	88.77(8)	O11–Zn2–O7	90.59(9)
O1–Zn1–N3	106.55(9)	O16–Zn2–N10	101.24(9)
O12–Zn1–N3	155.87(10)	O11–Zn2–N10	91.17(10)
O6–Zn1–N3	91.49(9)	O7–Zn2–N10	159.88(10)
O1–Zn1–N4	122.68(10)	O16–Zn2–N9	95.49(9)
O12–Zn1–N4	90.96(9)	O11–Zn2–N9	152.80(10)
O6–Zn1–N4	152.74(10)	O7–Zn2–N9	92.96(9)
N3–Zn1–N4	77.98(10)	N10–Zn2–N9	76.67(10)
Complex 3			
O6–Zn1–O11	101.82(9)	O17–Zn2–O12	93.93(9)
O6–Zn1–O1	91.84(9)	O17–Zn2–O22	96.88(10)
O11–Zn1–O1	94.87(9)	O12–Zn2–O22	97.12(10)
O6–Zn1–N1	159.62(9)	O17–Zn2–N7	163.97(10)
O11–Zn1–N1	98.09(10)	O12–Zn2–N7	89.90(9)
O1–Zn1–N1	90.81(9)	O22–Zn2–N7	98.09(11)
O6–Zn1–N2	93.29(9)	O17–Zn2–N8	92.81(10)
O11–Zn1–N2	104.28(9)	O12–Zn2–N8	152.79(9)
O1–Zn1–N2	158.69(9)	O22–Zn2–N8	108.19(10)
N1–Zn1–N2	77.47(10)	N7–Zn2–N8	77.07(10)

carboxylates have one shorter Zn–O and one longer Zn–O due to unequal distribution of electron density. In this complex zinc carries +2 charges which are balanced by carboxylate ligands.

3.3.2. Crystal structure of complex 2

Structural diagram of the complex 2 is shown in Fig. 2 and structural parameters in Table 3. The selected bond angles and lengths are presented in Tables 4 and 5. The complex is dinuclear with doubly bridged zinc ions each with square pyramidal geometry. The square base is formed by two carboxylate ligands and a bidentate bipyridine molecule. There are four carboxylate ligands

and two bipyridine molecules in the structure. The distance between two zinc ions of the molecule is 3.707 Å which is longer than 2.95 Å found in the tetra-bridged carboxylate zinc complex [27–30]. The bridged oxygen atom is slightly asymmetrically coordinated to the two zinc ions with 2.08 and 2.04 Å. The bipyridine moieties are coordinated with different bond lengths to both Zn atoms.

3.3.3. Crystal structure of complex 3

Structural diagram of the complex 3 is shown in Fig. 3 and structural parameters in Table 3. The selected bond angles and lengths are presented in Tables 4 and 5. Single crystal X-ray diffraction shows that complex 3 has monoclinic system with space group $P2_1/c$. The lattice contains two crystallographically different molecules as indicated by the different bond lengths and angles round zinc in both molecules. The separation between the two zinc ions of the two molecules is 7.197 Å. The central metal zinc is five coordinated as it is bonded with two oxygen atoms of two carboxylate ligand, two nitrogens of bipyridine and with one oxygen of water molecule. Both carboxylate ligands show a monodentate mode. The structural distortion index τ was used to determine the geometry of five coordinated compounds and calculated by $\alpha-\beta/60$ where α and β are the largest basal angles. The value of τ in this structure is 0.04 which indicates the geometry around zinc is slightly distorted square pyramidal because the value of τ for perfect square pyramidal is zero and for perfect trigonal bipyramidal is 1 [30]. This discrepancy occurs due to bulkiness of ligand or electron pair repulsion. In this complex again there is asymmetrical bond distance between zinc and nitrogens of bipyridine, their bond lengths are 2.106 and 2.114 Å. A water molecule is also present in crystal lattice which helps in the formation of more compact and packed structure by stabilizing the molecules through non-covalent interactions. One of the ligands in the crystallographically independent molecules of complex 3 is disordered with occupancy ratio of 0.501(10):0.499(10). This has been tackled partially with inclusion of restraints yielding satisfactory results. Benzene rings were treated as regular hexagons with C-atoms having equal anisotropic thermal parameters. Such explanation and resolution method has been applied for other complexes as well having crystallographically independent molecules in the unit cell [31].

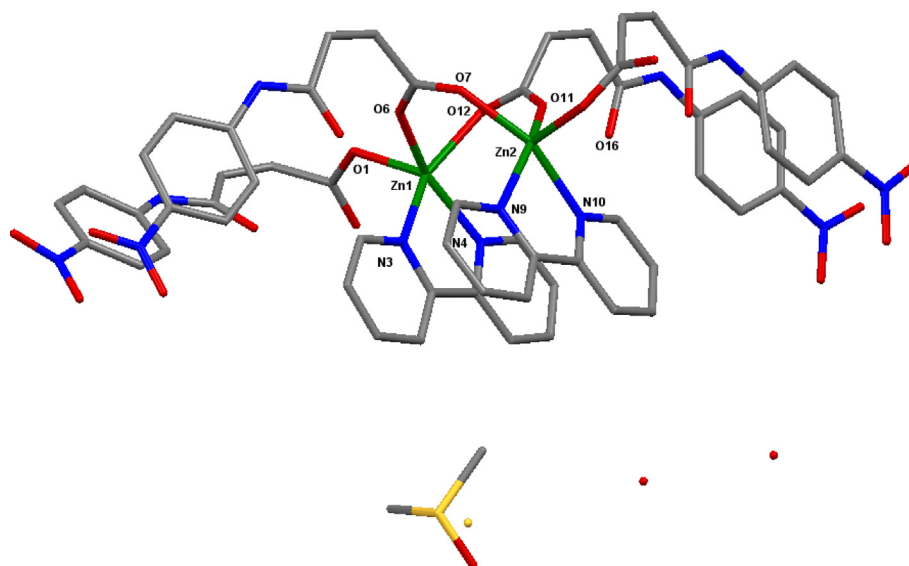


Fig. 2. Molecular diagrams of complex 2. H atoms are omitted for clarity. The red dots represent the oxygen atoms of water molecules. DMSO in distorted form is also present as solvent molecule. (Colour online.)

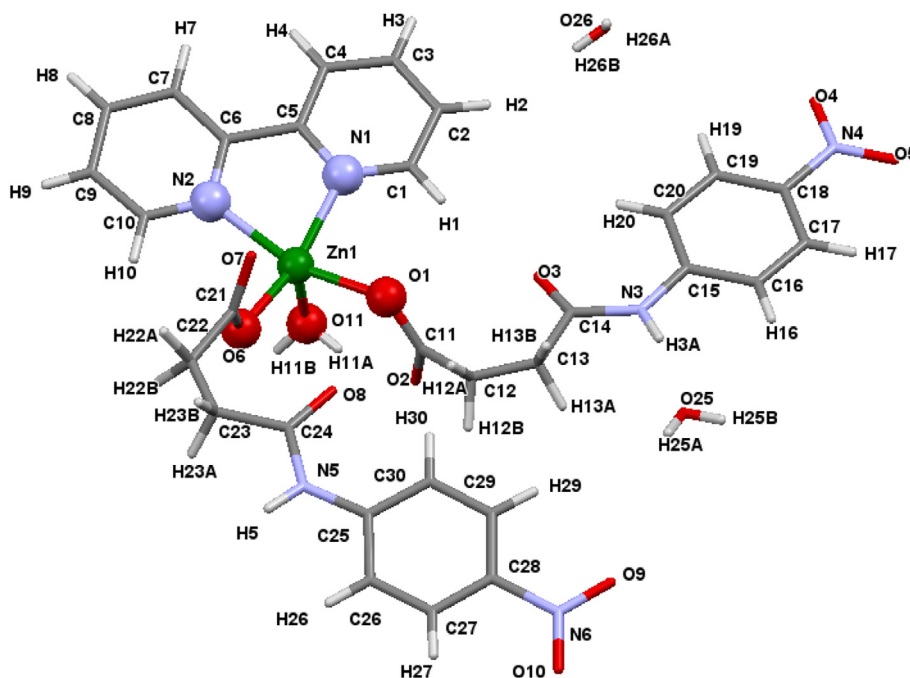


Fig. 3. Molecular diagrams of complex 3. One molecule is omitted from the unit cell for clarity.

3.4. UV-Visible spectroscopy

UV-Visible absorption spectroscopy is used to study the interaction of metal complexes with DNA. The study was performed by adding various concentrations of DNA to Zn complexes in order to monitor the change in the position of absorption bands as a result of some interaction between complex and DNA [34]. Absorption spectra of complexes 1–3 in the absence and presence of DNA are given in Figs. 4–6. A strong absorption band at 348.5–350 nm was appeared in the spectra of all the three complexes showing $\pi-\pi^*$ transitions due to aromatic ring present in their structures.

On addition of different concentrations of DNA, an obvious red shift of about 10 nm occurred in the absorption position showing some interaction between complex and DNA. Also with increase in concentration of DNA, absorption decreases which indicates the hypochromic effect. These two phenomena of red shift and hypochromic shift are the indication of intercalative mode of interaction [35–37].

Binding constant can be calculated by using Benesi-Hildebrand Eq. (1) [23] and to check the spontaneity of interaction between complex and DNA Gibb's free energy was calculated by using equation in (2).

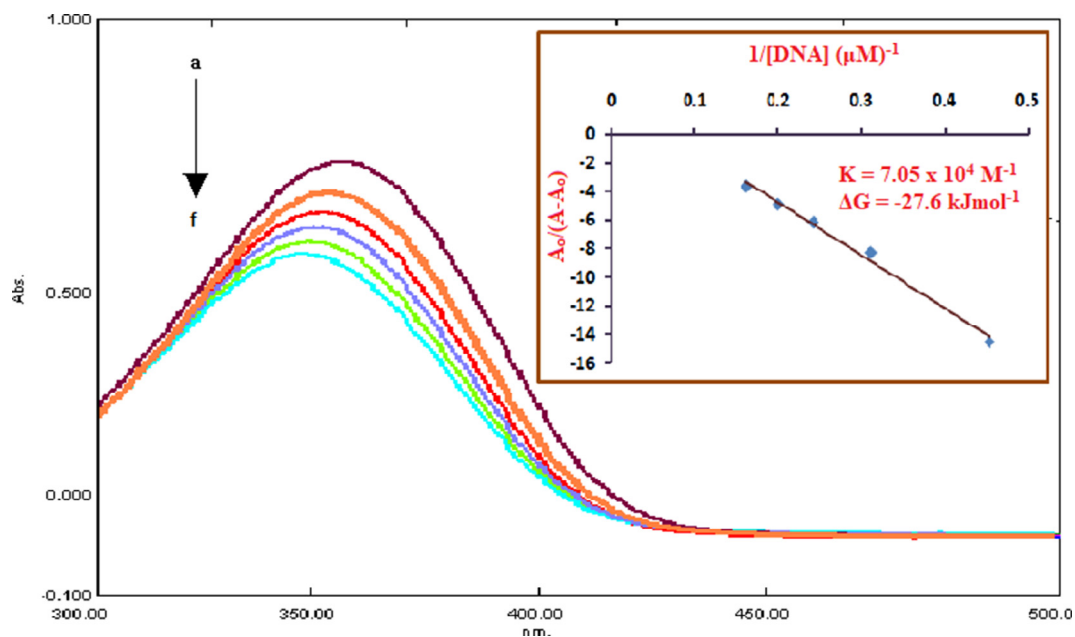


Fig. 4. Absorption spectrum of complex 1 in the absence (a) and presence of 1.17 μM (b), 2.2 μM (c), 3.21 μM (d), 4.317 μM (e), 5 μM (f) DNA. The arrow direction indicates increasing DNA concentration.

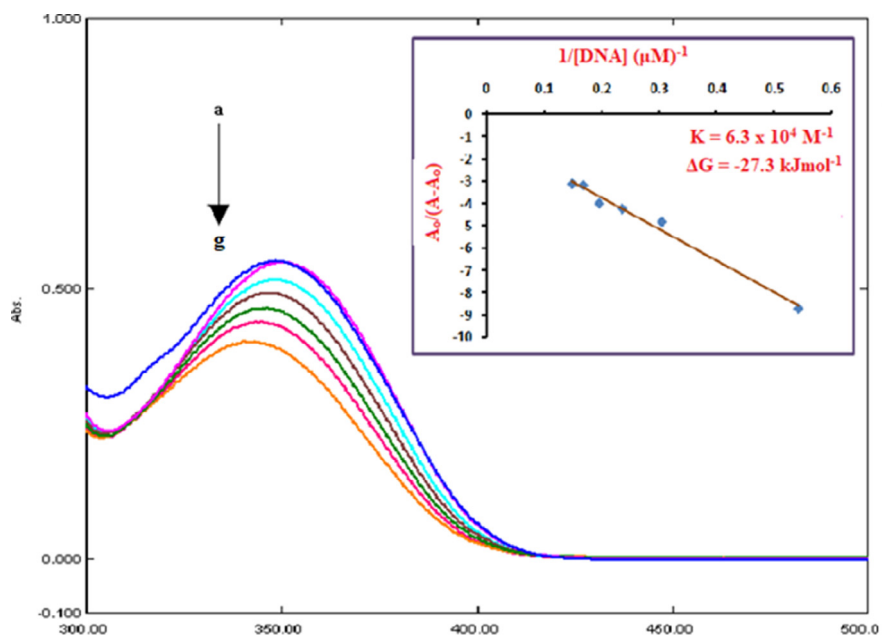


Fig. 5. Absorption spectrum of complex 2 in the absence(a) and presence of 11.17 μM (b), 2.2 μM (c), 3.21 μM (d), 4.317 μM (e), 5 μM (f) and 6 μM (g) DNA. Increase in DNA concentration is indicated by the direction of arrow.

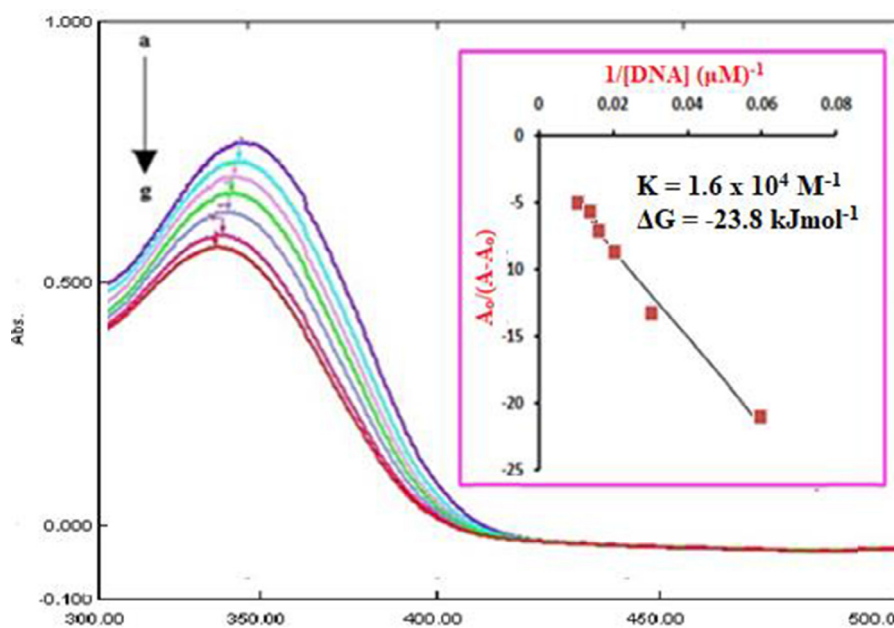


Fig. 6. Absorption spectrum of 0.5 mM complex 3 in the absence (a) and presence of 16.8 μM (b), 32 μM (c), 46.8 μM (d), 60.2 μM (e), 72.83 μM (f) and 87.4 μM (g) DNA.

$$\frac{A_0}{A - A_0} = \frac{\epsilon_G}{\epsilon_{H-G} - \epsilon_G} + \frac{\epsilon_G}{\epsilon_{H-G} - \epsilon_G} \cdot \frac{1}{K[DNA]} \quad (1)$$

Where K = binding constant, A and A₀ = Absorbances of drug-DNA solution and free drug solution, respectively.

ε_{H-G} and ε_G = molar absorption coefficients of drug-DNA and free drug, respectively.

K was obtained from slope to intercept ratio by plotting a graph between A₀/A-A₀ and 1/[DNA]

$$\Delta G = -RT \ln K \quad (2)$$

Where R = general gas constant (8.3141 J mol⁻¹ K⁻¹), K = binding constant and T = absolute temperature (298 K).

The value of K for complexes 1-3 are: 7.05 × 10⁴, 6.3 × 10⁴, 1.6 × 10⁴ M⁻¹ while the value Gibbs free energy are: ΔG = -27.6, -27.3, -23.8 kJmol⁻¹.

3.5. Viscosity measurements

Viscometric technique is also useful to investigate the binding modes of DNA with complexes. Change in viscosity determines

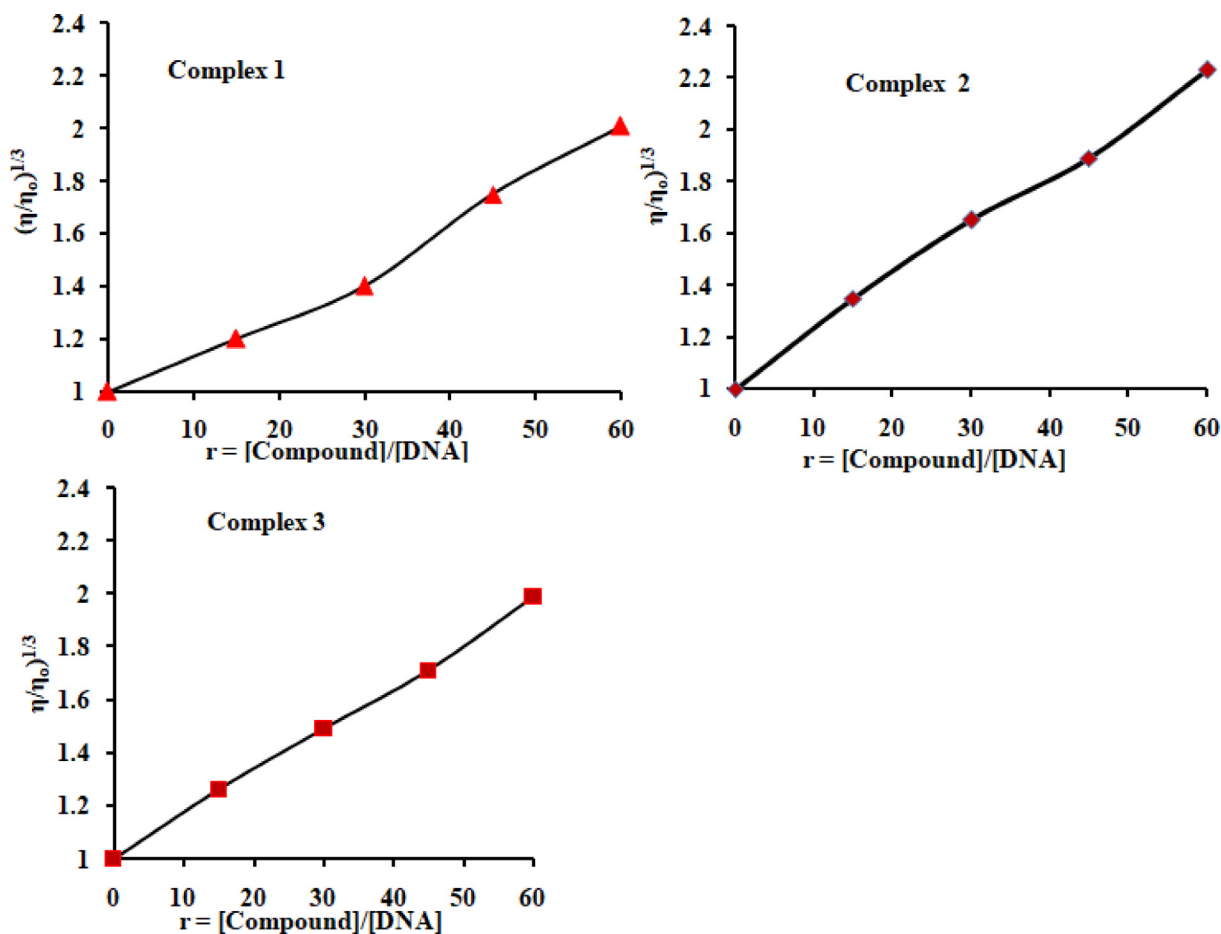


Fig. 7. Effect of increasing concentration of complexes 1–3 on relative viscosity of DNA at 25 ± 0.1 °C. [DNA] = 53×10^{-6} M.

the mode of binding. The viscosity of DNA is quite sensitive to chain length variation. In general, increase in viscosity indicates the intercalative mode of binding due to stacking of molecule between the nitrogenous bases causing lengthening of double helix so the viscosity of solution increases [38]. There is no significant change occurring in groove binding while in electrostatic binding mode slight decrease in viscosity takes place.

By the addition of different concentrations of complexes in DNA solution there was an increase in viscosity which indicates an intercalative mode of binding [39] as shown in Fig. 7.

Declaration of Competing Interest

The authors declare that they have no known competing financial interests or personal relationships that could have appeared to influence the work reported in this paper.

Acknowledgment

M. Iqbal gratefully acknowledges the Higher Education Commission (HEC) Islamabad, Pakistan (Grant No. 9257/KPK/NRPU/R&D/HEC/2017) for financial support.

Appendix A. Supplementary data

Supplementary data to this article can be found online at <https://doi.org/10.1016/j.poly.2019.114273>.

References

- [1] C.N.R. Rao, S. Natarajan, R. Vaidyanathan, *Angew. Chem., Int. Ed.* 43 (2004) 1466.
- [2] G. Blay, I. Fernandez, T. Gimenez, J.R. Pedro, R. Ruiz, E. Prdo, F. Lloret, M.C. Munoz, *Chem. Commun.* (2001) 2102.
- [3] Q. Chu, G.X. Liu, Y.Q. Huang, X.F. Wang, W.Y. Sun, *J. Chem. Soc., Dalton Trans.* (2007) 4302.
- [4] P.G. Lassahn, V. Lozenge, G.A. Timco, P. Christian, C. Janiak, R.E.P. Winpenny, *J. Catal.* 222 (2004) 260.
- [5] M.L. Tong, S. Hu, J. Wang, S. Kitagawa, S.W. Ng, *Cryst. Growth Des.* 5 (2005) 837.
- [6] J.C. Dai, X.T. Wu, Z.Y. Fu, C.P. Cui, S.M. Hu, W.X. Du, L.M. Wu, H.H. Zhang, R.Q. Sun, *Inorg. Chem.* 41 (2002) 1391.
- [7] M.C. Hong, Y.J. Shako, W.P. Su, R. Cao, M. Fujita, Z.Y. Zhou, A.S.C. Chan, *Angew. Chem., Int. Ed.* 39 (2000) 2468.
- [8] N. Matsumoto, Y. Motoda, T. Matsuo, T. Nakashima, N. Re, F. Dahan, J.P. Tuchagues, *Inorg. Chem.* 38 (1999) 1165.
- [9] O.S. Jung, S.H. Park, K.M. Kim, H.G. Jang, *Inorg. Chem.* 37 (1998) 5781.
- [10] R.W. Saalfrank, I. Bernt, M.M. Chowdhury, F. Hammel, G.B.M. Vaughan, *Chem. Eur. J.* 7 (2001) 2765.
- [11] G.B. Deacon, R.J. Phillips, *Coord. Chem. Rev.* 33 (1980) 227.
- [12] C. Hou, Q. Liu, Y. Lu, T. Okamura, P. Wang, M. Chen, W.Y. Sun, *Micropor. Mesopor. Mater.* 152 (2012) 96.
- [13] S. Prasad, J.T. Ananda, B. Fitzgerald, B. Bao, F.W.J. Beck, P.H. Chandrasekar, *Ann. Intern. Med.* 133 (2000) 245.
- [14] N. Uddin, M. Sirajuddin, N. Uddin, H. Ullah, S. Ali, M. Tariq, S.A. Tirmizi, A.R. Khan, *Spectrochim. Acta A* 140 (2015) 563.
- [15] J. Fielden, P.T. Gunning, D.L. Long, M. Nutley, A. Ellern, P. Kögerler, L. Cronin, *Polyhedron* 25 (2006) 3474.
- [16] P.L. Ng, C.S. Lee, H.L. Kwong, A.S.C. Chan, *Inorg. Chem. Commun.* 8 (2005) 769.
- [17] Y.C. Shen, Z.J. Li, J.K. Cheng, Y.Y. Qin, Y.G. Yao, *Inorg. Chem. Commun.* 10 (2007) 888.
- [18] N. Muhammad, M. Ikram, A. Wadood, S. Rehman, S. Shujah, Erum, M. Ghufuran, S. Rahim, M. Shah, C. Schulzke, *Spectrochim. Acta Part A* 190 (2018) 368.
- [19] D.K. Mishra, U.K. Singha, A. Das, S. Dutta, P. Kar, A. Chakraborty, A. Sen, B. Sinha, *J. Coord. Chem.* 14 (2018) 2165.
- [20] M. Sirajuddin, S. Ali, A. Badshah, *J. Photochem. Photobiol. B* 124 (2013) 1.

- [21] G.M. Sheldrick, A short history of SHELX, *Acta Crystallogr. Sect. A* 64 (2007) 112.
- [22] M. Sirajuddin, S. Ali, V. McKee, S. Zaib, J. Iqbal, *RSC Adv.* 4 (2014) 57505.
- [23] H.A. Benesi, J. Hildebrand, *J. Am. Chem. Soc.* 71 (1949) 2703.
- [24] M. Sirajuddin, V. McKee, M. Tariq, S. Ali, *Eur. J. Med. Chem.* 143 (2018) 1903.
- [25] M. Sirajuddin, S. Ali, N.A. Shah, M.R. Khan, M.N. Tahir, *Spectrochim. Acta Part A* 94 (2012) 134.
- [26] S. Mathur, S. Tabassum, *Cent. Eur. J. Chem.* 4 (2006) 502.
- [27] V. Zelenak, Z. Vargov, K. Gyoryov, *Spectrochim. Acta, Part A* 66 (2007) 262–272.
- [28] R. Sarma, J.B. Baruah, *Solid State Sci.* 13 (2011) 1692.
- [29] M. Iqbal, S. Ali, M. Sohail, M.N. Tahir, P.A. Anderson, *J. Chin. Chem. Soc.* (2019) 1.
- [30] K. Ullah, M. Sirajuddin, M. Zubair, A. Haider, S. Ali, F. Ullah, G. Dutkiewicz, M. Kubicki, C. Rizzoli, *J. Iran. Chem. Soc.* 16 (2019) 1163.
- [31] M. Zubair, M. Sirajuddin, A. Haider, K. Ullah, I. Ullah, A. Munir, S. Ali, M.N. Tahir, *J. Mol. Struct.* 428 (2018) 567.
- [32] S. Jin, D. Wang, *Inorg. Chim. Acta* 415 (2014) 31.
- [33] K. Hu, S. Jin, Z. Xie, M. Guo, Z. Lin, D. Wang, *Polyhedron* 139 (2018) 17.
- [34] M. Sirajuddin, S. Ali, V. McKee, A. Wadood, M. Ghufan, *J. Mol. Struct.* 1181 (2019) 93.
- [35] E.C. Long, J.K. Barton, *Acc. Chem. Res.* 23 (1990) 271.
- [36] M. Sirajuddin, N. Uddin, S. Ali, M.N. Tahir, *Spectrochim. Acta A* 116 (2013) 111.
- [37] M. Sirajuddin, S. Ali, V. McKee, H. Ullah, *Spectrochim. Acta A* 138 (2015) 569.
- [38] S. Murtaza, S. Shamim, N. Kousar, M.N. Tahir, M. Sirajuddin, U.A. Rana, *J. Mol. Struct.* 1107 (2016) 99.
- [39] R.A. Hussain, A. Badshah, M. Sohail, *J. Mol. Struct.* 1048 (2013) 367.